Reaction conditions effect and pathways in the oxidative steam reforming of raw bio-oil on a Rh/CeO2-ZrO2 catalyst in a fluidized bed reactor

Arandia, Aitor; Remiro, Aingeru; Oar-Arteta Gonzalez, L.; Bilbao, Javier; Gayubo, Ana G.

DOI
10.1016/j.ijhydene.2017.10.095

Publication date
2017

Document Version
Accepted author manuscript

Published in
International Journal of Hydrogen Energy

Reaction conditions effect and pathways in the oxidative steam reforming of raw bio-oil on a Rh/CeO_2-ZrO_2 catalyst in a fluidized bed reactor

Aitor Arandia[a], Aingeru Remiro[a,*], Lide Oar-Arteta[b], Javier Bilbao[a], Ana G. Gayubo[a]

[a]*Chemical Engineering Department, University of the Basque Country, P. O. Box 644, 48080. Bilbao, Spain.*

[b]*Catalysis Engineering / ChemE / TUDelft, Van der Maasweg 9, 2629 HZ Delft (The Netherlands)*

**email: aingeru.remiro@ehu.eus Phone: +34 946 015361. Fax: +34 946 013 500*

Abstract

A reaction scheme has been proposed for the oxidative steam reforming (OSR) of raw bio-oil on a Rh/CeO_2-ZrO_2 catalyst, based on the study of the effect reaction conditions (temperature, space time, oxygen/carbon ratio and steam/carbon ratio) have on product yields (H_2, CO, CO_2, CH_4, hydrocarbons). The runs were performed in a two-step system, with separation of pyrolytic lignin (first step) followed by catalytic reforming in a fluidized bed reactor (second step), under a wide range of reaction conditions (600-750 ºC; space time, 0.15-0.6 $g_{catalyst}h/g_{bio\text{-}oil}$; oxygen to carbon molar ratio (O/C), 0-0.67; steam to carbon molar ratio (S/C), 3-9). The catalyst is very active for bio-oil reforming, and produces high H_2 yield (between 0.57 and 0.92), with low CO yield (0.035-0.175) and CH_4 yield (below 0.045) and insignificant light hydrocarbons formation. The proposed reaction scheme considers the catalyzed reactions (reforming, water gas shift (WGS) and combustion) and the thermal routes (decomposition/cracking and

combustion). The deactivation of the catalyst affects progressively the reactions in the following order: CH_4 reforming, hydrocarbons reforming, oxygenates reforming, combustion and WGS.

(Keywords: bio-oil, oxidative steam reforming, hydrogen, Rh catalyst, reaction scheme

1. Introduction

Environmental problems arising from the use of fossil fuels to meet the growing energy demand boost the development of sustainable fuel production processes from renewable energy sources [1]. In this context, H_2 plays an important role as a clean energy carrier (with increasing demand for its use in fuel cells) and as a raw material in petrochemical industry and agrochemistry [2,3]. Great attention has been paid to H_2 production from biomass as raw material because it does not contribute to CO_2 generation [4,5].

Hydrogen production routes from biomass can be classified into: i) direct routes, such as gasification, high-temperature pyrolysis, catalytic pyrolysis and biological processes [6,7]; and ii) indirect routes, such as the reforming of biomass-derived oxygenates, e.g. bio-oil [8,9]. Bio-oil (the liquid product from fast pyrolysis of lignocellulosic biomass) can be obtained with high yields from different types of biomass, by means of decentralized small-scale units with simple design and environmentally friendly [10-12]. It can be subsequently transported to a centralized factory for H_2 generation more economically than biomass, due to its lower volume and higher energy density [13]. Consequently, the reforming of bio-oil is a process with good prospects for a large scale H_2 production and it is considered one of the most economically feasible methods to produce high purity hydrogen [14,15]. Moreover, the economy of H_2 generation will be favored when it is produced at large scale [8].

An attractive aspect of steam reforming (SR) of bio-oil is the fact that it does not require the previous dehydration of bio-oil [16]. It is a highly endothermic reaction, which proceeds according to the stoichiometry of Eq. (1). Considering the water-gas-

shift (WGS) reaction, Eq. (2), which takes place with the excess water in the reaction medium, the overall reaction for SR of bio-oil can be represented by Eq. (3) [17,18].

$$C_nH_mO_k + (n-k)\ H_2O \rightarrow n\ CO + (n+(m/2) - k)\ H_2 \quad (1)$$

$$CO + H_2O \leftrightarrow CO_2 + H_2 \quad (2)$$

$$C_nH_mO_k + (2n-k)\ H_2O \rightarrow\ n\ CO_2 + (2n+m/2-k)\ H_2 \quad (3)$$

Bio-oil is a complex mixture of oxygenates and water and due to the high temperature needed to reform the heavy oxygenates, undesired parallel reactions occur, such as decomposition/cracking reactions, Eq. (4), and reverse water gas-shift reaction (r-WGS, reverse of Eq. (2)), which consumes H_2 and increases CO production [19,20].

$$C_nH_mO_k \rightarrow C_xH_yO_z + \text{gases } (H_2, CO, CO_2, CH_4) + \text{coke} \quad (4)$$

The main challenges for the industrial implementation of bio-oil SR are the high energy supply required (due to its endothermic nature and the need for vaporizing a great amount of water) and the rapid catalyst deactivation by coke deposition, associated with the capacity for re-polymerization of the phenolic compounds in bio-oil [21]. In order to overcome the energy requirement, oxidative steam reforming (OSR), with both O_2 and steam in the feed, is an interesting alternative. Thus, in the OSR, energy is supplied by the partial oxidation of the compounds in the reaction medium, and with an appropriate O/S(steam)/C ratio autothermal reforming (ATR) regime is achieved [22,23]. Moreover, the co-feeding of O_2 promotes the combustion of the carbonaceous deposits (coke), which delays deactivation and enlarges catalyst lifetime [24,25]. Nevertheless, in spite of these advantages with respect to SR, the OSR process has the inconvenience of a lower H_2 yield (due to the partial combustion of the oxygenated compounds and of the H_2 in the reaction medium), according to the global stoichiometry given by Eq. (5). Thus, a thermodynamic analysis of the autothermal

reforming of selected compounds of bio-oil revealed 20 wt% lower H_2 yield (in the optimum conditions) compared to SR process [26].

$$C_nH_mO_k + pO_2 + (2n-k-2p)H_2O \rightarrow nCO_2 + (2n+m/2-k-2p)H_2 \quad (5)$$

Due to the suitable activity-cost balance, Ni based catalyst have been widely studied in the SR and OSR of methane and hydrocarbons [27,28], pure oxygenates [16,24,29-33], bio-oil aqueous fraction [18,20,23,34,35], and, to a lower extent, in the SR of raw bio-oil [17,36,37]. In spite of their high cost compared to Ni based catalysts, noble-metal based catalysts have also been extensively studied for SR and OSR of pure oxygenated compounds, mainly ethanol, [38-45].

Better performance of Rh based catalysts compared to Ni based catalysts was proven in the OSR of ethanol [39] and glycerol [41], and the improvement of a Ni catalyst by promoting it with Rh has been also reported in the OSR of bio-ethanol [46]. Nevertheless, the studies on bio-oil reforming with noble-metal catalysts, and especially those concerning OSR are scarce [22,47,48]. In a recent work [49], we have proven the better performance of a commercial Rh/CeO_2-ZrO_2 catalyst in the OSR of raw bio-oil than a Ni/La_2O_3-αAl_2O_3 catalyst previously used for the SR of bio-oil [17,18,20]. On the one hand, Rh/CeO_2-ZrO_2 catalyst is more active and selective than Ni/La_2O_3-αAl_2O_3, which allows obtaining higher H_2 yield and lower CO yield due to its higher activity for the WGS reaction. On the other hand, Rh/CeO_2-ZrO_2 catalyst is more stable than Ni/La_2O_3-αAl_2O_3 catalyst at the studied temperature (700 ºC), which is explained by the lower formation of encapsulating coke for the Rh, and because Rh does not undergo sintering under OSR conditions.

Given the good performance of the Rh/CeO_2-ZrO_2 catalyst in the OSR of raw bio-oil, the aim of this work is to delimit the suitable reaction conditions range for this catalyst

and also establish a kinetic scheme that considers the different reaction steps (thermal and catalytic) and explains the effect of reaction conditions on individual products yields. For that purpose, the OSR of raw bio-oil has been studied under a wide range of reaction conditions (temperature, space time, oxygen/steam/carbon molar ratios in the feed). In order to assess the significance of thermal routes (mainly by oxygenates decomposition) on bio-oil conversion and products distribution, some runs without catalyst have been also performed. Moreover, the catalyst stability has been tested by means of a run at low temperature (600 ºC, at which deactivation is fast) with the aim of establishing differences in the deactivation rate among the catalytic routes (reforming, combustion and WGS). The runs have been carried out in an equipment with two steps in series, which is suitable for minimizing catalyst deactivation in the up-grading of raw bio-oil [17,18,20,50,51]. In the first step (at 500 ºC, without catalyst) the pyrolytic lignin (formed by re-polymerization of phenolic compounds in bio-oil, derived from lignin pyrolysis) is retained, and the remaining oxygenates are reformed in the second step (fluidized reactor bed).

2. Materials and Methods

2.1. Catalysts

The commercial Rh/CeO_2-ZrO_2 catalyst (with 2 wt % Rh content, denoted as Rh/ZDC), was supplied by *Fuel Cell Materials*. The physical properties (determined by N_2 adsorption-desorption) are: specific BET surface area, 85.7 m^2g^{-1}; average pore diameter, 17.7 nm, and; pore volume, 0.31 cm^3g^{-1}. The metallic properties (determined by CO chemisorption) are: metal dispersion, 72.5 %; metallic surface area of 319 $m^2g_{metal}^{-1}$. The TPR profile shows that Rh_2O_3 is completely reduced below 250 ºC in a flow of 10 % H_2/Ar mixture. The presence of Ce and Zr oxides was confirmed by XRD

analysis, but no diffraction peaks corresponding to Rh_2O_3 (prior to reduction) or Rh^0 (after reduction) were observed, due to the low Rh content and its high dispersion on the support [49]. The Rh particle size has been estimated from TEM images (Figure 1), with a particle size distribution from 1 to 2.5 nm (inserted window in Figure 1).

Figure 1

2.2. Bio-oil production and composition

The raw bio-oil was obtained by flash pyrolysis of pine sawdust at 480 ºC in a demonstration plant (Ikerlan-IK4 technology center, Alava (Spain), with a biomass feeding capacity of 25 kg/h) [52], which was developed based on results obtained in a laboratory plant (120 g/h) with a conical spouted bed reactor [53,54]. The water content of the bio-oil is 38 wt%, its density is 1.107 g ml^{-1} and the empiric formula obtained by CHO analysis is $C_{4.21}H_{7.14}O_{2.65}$. The raw bio-oil composition, determined by GC/MS analyser (*Shimadzu QP2010S device*) is shown in a previous work [49].

2.3. Reaction equipment and operating conditions

Runs have been performed in an automated reaction equipment of stainless steel (*MicroActivity Reference* from *PID Eng&Tech*) provided with two units in series (thermal step and catalytic step), which has been previously described in detail [49]. In the thermal step (U-shaped tube, at 500 ºC) around 11 wt % of the raw bio-oil oxygenates was deposited as pyrolytic lignin. The corresponding molecular formula of the bio-oil exiting the thermal step is $C_{3.8}H_{7.7}O_{2.9}$ (water-free basis, calculated from a mass balance, taking into account the molecular formula of the raw bio-oil and the amount and composition of the pyrolytic lignin deposited). In the second unit (reforming reactor in fluidized bed regime), the catalyst is mixed with inert solid (SiC) (inert/catalyst mass ratio > 8/1) in order to assure a correct fluidization regime. Prior to

each reforming reaction, the catalyst is reduced in-situ in H_2-N_2 stream (10 vol % H_2) at 700 ºC for 2 h. The reactions have been carried out at atmospheric pressure and with the following ranges of the remaining reaction conditions: 600-750 ºC; space time, 0.15-0.6 $g_{catalyst}h/g_{bio\text{-}oil}$; steam/carbon (S/C) molar ratio, 3-9; oxygen/carbon ratio (O/C), 0-0.67 (the last one corresponding to autothermal regime). The bio-oil (0.08 ml/min) is fed with a *Harvard Apparatus 22 injection pump*, and the water flow rate corresponding to each S/C molar ratio is co-fed with a *307 Gilson pump*. O_2 is co-fed at the entrance of the second step (fluidized bed reactor), in order to avoid the combustion of oxygenates in the first step (thermal treatment), thus maximizing the H_2 yield in the two step reaction system [55].

The products stream is analysed in-line with a *MicroGC 490* from *Agilent*, equipped with 4 analytic channels: molecular sieve MS5 for quantifying H_2, N_2, O_2, CH_4 and CO; Plot Q for CO_2, H_2O and C_2-C_4 hydrocarbons; CPSIL for C_5-C_{11} hydrocarbons (not detected in this study), and; Stabilwax for oxygenated compounds.

2.4. Reaction indices

The kinetic behaviour has been quantified with the following reaction indices:

Bio-oil conversion: $$X_{bio\text{-}oil} = \frac{F_{in} - F_{out}}{F_{in}} \quad (6)$$

where F_{in} and F_{out} are the molar flow rate of bio-oil at the reactor inlet and outlet, respectively, in C units contained.

H_2 yield: $$Y_{H_2} = \frac{F_{H_2}}{F^{o}_{H_2}} \quad (7)$$

where F_{H2} is the H_2 molar flow rate in the product stream and F^{o}_{H2} is the stoichiometric molar flow rate, which has been evaluated for the SR reaction as $[(2n+m/2-k)/n]\ F_{in}$,

according to Eq. (1). Taking into account the molecular formula of the bio-oil entering the reforming reactor ($C_{3.8}H_{7.7}O_{2.9}$), the value of F°_{H2} is $2.25F_{in}$.

Yield of C-containing products (CO_2, CO, CH_4 and light hydrocarbons):

$$Y_i = \frac{F_i}{F_{in}} \quad (8)$$

where F_i is the molar flow rate of each compound, in C units contained.

3. Results and Discussion

3.1. Contribution of thermal routes

With the aim of assessing the significance of the thermal routes in bio-oil conversion and products yields at the fluidized bed reactor outlet, the effect of temperature and O/C molar ratio in non-catalytic reforming runs (blank runs without catalyst) has been studied. The runs have been carried out in the following conditions: 500-750 ºC range; O/C ratio: 0-0.67; S/C ratio of 6. The effect of temperature (at O/C = 0.34) and O/C ratio (at 700 ºC) on the bio-oil conversion and products yields (H_2, CO, CO_2, CH_4 and C_2-C_4 hydrocarbons (denoted HCs)) is shown in Figure 2.

Figure 2

In Figure 2a, the results corresponding to a run at 500 ºC without O_2 (O/C = 0) have been included. In these conditions, H_2, CH_4, hydrocarbons, CO_2 and CO are produced by thermal decomposition of oxygenates (cracking/decarboxylation/decarbonilation reactions). Comparing these results for O/C = 0 with those corresponding to O/C = 0.34 at the same temperature, it is observed that the presence of O_2 in the reaction medium favors bio-oil conversion, thereby increasing CO and CO_2 yields, which should be attributed to the promotion of partial combustion of oxygenates. This hypothesis is coherent with the lower yields of H_2 and hydrocarbons due to their partial combustion. Nevertheless, CH_4 yield is hardly affected by combustion at this temperature.

The results in Figure 2a for O/C = 0.34 give evidence that for a reaction medium with O_2, the bio-oil conversion increases with temperature, although this effect is progressively attenuated. The yields of products also increase with temperature, except CO_2 yield, which is maximum at 600 ºC. The higher concentration of H_2, CH_4 and hydrocarbons indicates that temperature favors the oxygenates decomposition/cracking reactions over their partial combustion. Moreover, the higher increase in the yields of CO and CO_2 over the rest of products can be attributed to a higher extent of combustion reactions and/or decarboxylation/decarbonilation of oxygenates when temperature is increased. However, the decrease in CO_2 yield above 600 ºC evidences that in these conditions (> 600 ºC and low O_2 concentration, O/C = 0.34) the increase in temperature selectively favors incomplete combustion reactions and/or decarbonilation of oxygenates over total combustion and/or decarboxylation.

The comparison of the values of bio-oil conversion and products yields for different O/C ratios at the same temperature (Figure 2b) allows establishing a relationship between the results and the extent of the combustion reactions of oxygenates and products, assuming that O/C ratio has low effect on decomposition reactions. Thus, with the increase in O/C ratio the yields of CH_4 and hydrocarbons decrease due to their combustion, and H_2 yield decreases to a lower extent. The steady increase in CO_2 yield and the slight maximum for CO yield prove that total combustion of oxygenates is favored for a high O/C ratio, so that CO_2 is the major product for O/C = 0.67.

3.2. Catalytic routes. Effect of reaction conditions

The afore-mentioned results give evidence of the importance of thermal routes in the absence of catalyst. However, with a catalyst the reaction rate of the catalyzed routes (reforming, combustion and WGS) is promoted and the significance of the thermal

routes decreases considerably. Consequently, the catalytic routes have a higher effect on the results, and they are mainly associated with the extent of these routes.

The role of catalytic routes in the wide range of reaction conditions studied can be determined from the results in Figures 3-6, corresponding to the effect of space time, temperature, O/C ratio and S/C ratio, respectively. It should be pointed out that total conversion of bio-oil has been obtained at zero time in all the studied reaction conditions.

In Figure 3, the results obtained without catalyst have been included. A comparison of the results with and without catalyst at 600 ºC (Figure 3a) and 700 ºC (Figure 3b), shows that the presence of the catalyst modifies noticeably products distribution due to the promotion of reforming reactions (involving oxygenates, and the CH_4 and hydrocarbons formed by oxygenates decomposition) and WGS reaction. Therefore, high H_2 and CO_2 yields are obtained (0.76 and 0.96, respectively for a low space time value of 0.15 $g_{catalyst}h/g_{bio\text{-}oil}$), and low CO yield (0.05). These yields hardly change when space time is four times higher, which indicates that they are close to the thermodynamic equilibrium and proves that the catalyst is very active for reforming and WGS reactions. The effect of space time is qualitatively similar at 700 ºC (Figure 3b), although H_2 yield is slightly lower than that corresponding to 600 ºC. CO_2 yield is also lower, but CO yield is higher.

Figure 3

In Figure 4 the effect of reforming temperature on reaction indices is shown for two values of space time. The hydrocarbons yield is not shown because it is not significant.

For the highest space time value (Figure 4a), and consequently for a high extent of catalytic reactions, the yields of H_2 and CO_2 slightly decrease when temperature is

increased, whereas the yield of CO increases, because the r-WGS reaction is thermodynamically favored. The yield of CH_4 is very low and decreases with temperature, because its reforming is favored. It should be pointed out the low decrease in H_2 yield (from 0.76 to 0.75) in the 600-750 ºC range, which indicates that its combustion is not significantly favored by the increase in temperature. This low effect of temperature was also observed by Rioche et al. [47] in the OSR of model compounds (acetone, acetic acid, ethanol and phenol) with a 1%Rh/$CeZrO_2$ catalyst.

The fact that combustion does not significantly affect H_2 yield shows that this catalyst is interesting for the OSR of bio-oil, due to the selective promotion of reforming and WGS reactions over those of combustion.

For a low space time value (0.15 $g_{catalyst}h/g_{bio\text{-}oil}$, Figure 4b), the H_2 and CO_2 yields are lower and CO yield is higher than those in Figure 4a, as a consequence of the lower extent of reforming and WGS reactions. The effect of the increase in temperature is qualitatively similar to that observed in Figure 4a, with a slightly higher decrease in H_2 yield (from 0.75 to 0.72) when temperature is increased from 600 to 700 ºC.

Figure 4

The O/C ratio has a higher effect on products yield than space time and temperature, as observed in Figure 5. In this Figure, each graph corresponds to a given value of the remaining reaction conditions (temperature, space time and S/C ratio), taken as an example. In both reaction conditions, the yields of H_2, CO and CH_4 decrease and that of CO_2 increases when the O/C ratio is increased, because the extent of combustion reactions (of oxygenates in bio-oil and of reaction products) is favored. In the conditions of Figure 5a (600 ºC, 0.6 $g_{catalyst}h/g_{bio\text{-}oil}$, S/C = 6) the H_2 yield decreases almost linearly from 0.91 to 0.58 when O/C ratio increases from 0 (SR conditions) to

0.67 (ATR conditions). This noticeable decrease in H_2 yield, and the small change in CO_2 and CO yields, evidences a selective combustion of H_2 compared to that of the carbon products (oxygenates, CH_4 and CO).

At higher temperature (700 ºC) and lower value of space time (0.15 $g_{catalyst}h/g_{bio\text{-}oil}$) (Figure 5b) the effect of O/C ratio is qualitatively similar to the aforementioned in Figure 5a. Nevertheless, by comparing the results in Figures 5a and 5b in the conditions of autothermal reforming (O/C = 0.67), it is observed that the H_2 yield obtained at high temperature and low space time (700 ºC and 0.15 $g_{catalyst}h/g_{bio\text{-}oil}$, Figure 5b) is higher than that obtained at low temperature and high space time (600 ºC and 0.6 $g_{catalyst}h/g_{bio\text{-}oil}$, Figure 5a). This result evidences the interest of this catalyst for the ATR of bio-oil, because reforming and WGS reactions are faster than H_2 combustion reaction and, moreover, the former are selectively favored by the increase in temperature.

Figure 5

The afore mentioned results of decrease in H_2 yield when O/C ratio is increased are coherent with those observed by Rioche et al. [47] in the reforming of a raw bio-oil (obtained by the fast pyrolysis of beech wood) with 1%Pt/$CeZrO_2$ catalyst at 860 ºC.

The effect of steam/carbon (S/C) molar ratio on products yield is shown in Figure 6 for two reaction conditions. Graph a corresponds to 600 ºC, O/C ratio of 0.34 and space time of 0.6 $g_{catalyst}h/g_{bio\text{-}oil}$. Graph b corresponds to the same O/C ratio and different values of temperature and space time (700 ºC and 0.15 $g_{catalyst}h/g_{bio\text{-}oil}$, respectively). As observed in Figure 6a, H_2 and CO_2 yields increase noticeably (in the 0.63-0.83 and 0.85-0.96 ranges, respectively) when S/C ratio is increased from 3 to 9, whereas CO and CH_4 yields decrease (in the 0.08 - 0.04 and 0.045 - 0.01 ranges, respectively).

Figure 6

The results for other reaction conditions (Figure 6b) are qualitatively similar, but with different values of products yields due to the differences in the relative extent of the reactions. Thus, in Figure 6b the range of H_2 yield is narrower than that observed in Figure 6a and, moreover, the yields of CO_2 and CO are lower and higher, respectively. These differences are related to two effects: on the one hand, the higher extent of WGS reaction in the conditions of Figure 6a (higher value of space time than in Figure 6b) and, on the other hand, the WGS reaction is thermodynamically favored (lower temperature).

The favorable effect of increasing S/C ratio on H_2 yield is well documented in literature for the SR of different feeds on different catalysts [17,20,32,56,57], although it has the inconvenience of a higher energy requirement. For a low space time value (0.15 $g_{catalyst}h/g_{bio\text{-}oil}$, Figure 6b), which corresponds to kinetic control regime, the variation in the yields of H_2, CO_2 and CO is almost linear with S/C ratio. Nevertheless, for a high space time value (Figure 6a), which corresponds to thermodynamic control regime, the increase in H_2 and CO_2 yields and decrease in CO yield are attenuated above S/C = 6. Consequently, and intermediate value of S/C ratio, close to 6, will be suitable for the OSR of bio-oil, in order to achieve a compromise between H_2 yield and energy required for vaporizing the water in the feed.

3.3. Selective deactivation of the catalyst

In addition to the lower energy requirement, one of the expected advantages of bio-oil OSR compared to SR is the attenuation of deactivation by coke, as proven in a previous work in which the importance of O/C ratio on coke formation was determined [49]. Thus, at 700 ºC the main cause of catalyst deactivation in the SR was the deposition of encapsulating coke that blocked Rh sites, but under OSR conditions (with

presence of O_2 in the reaction medium) the deactivation of Rh/ZDC catalyst was very slow due to the effective combustion of coke precursors. Furthermore, the used catalyst showed a slight change in Rh oxidation state (which was proven by means of Temperature Programmed Reduction (TPR) analysis). Consequently, under OSR conditions, there was an initial period of deactivation, with a small decrease in activity, and subsequently bio-oil conversion and the yields of H_2 and carbon products kept constant along a period of time depending on the reaction conditions [49].

In this work, the aim is to analyze the effect catalyst deactivation has on products yield. For that purpose, the results in Figure 7 correspond to a run under fast deactivation conditions, with a relatively short time on stream (10 h) but enough for determining the effect of deactivation on the different reactions of the kinetic scheme. These reaction conditions are: 600 ºC; 0.6 $g_{catalyst}h/g_{bio\text{-}oil}$; O/S/C molar ratio of 0.34/6/1.

As observed in Figure 7, Rh/ZDC catalyst is stable for 200 min time on stream, with total bio-oil conversion and H_2 yield close to 0.8. Moreover, CH_4 yield is lower than 0.01 and the formation of hydrocarbons is insignificant. Subsequently, a sequence of changes in bio-oil conversion and products yield occur, that can be attributed to the existence of several catalyst deactivation causes, which have different kinetics and affect differently to the reactions in the kinetic scheme [49].

Thus, after 200 min time on stream a decrease in H_2 and CO_2 yields and an increase in CH_4 yield is observed, which evidences the selective deactivation of CH_4 reforming reaction.

Figure 7

Subsequently, after 300 min a decrease in bio-oil conversion is observed, together with a more pronounced decrease in the H_2 and CO_2 yields, and a parallel increase in

hydrocarbons yield. These phenomena should be attributed to the deactivation of the catalyst for oxygenates reforming and combustion reactions (decrease in conversion) and hydrocarbons reforming (increase in their yield). Subsequent to 400 min time on stream, the catalysts is almost totally deactivated for CH_4 and hydrocarbons reforming reactions, and the yields of these products are almost equal to those obtained without catalyst at the same temperature (Figure 2a). Also, the faster decrease in H_2 yield compared to CO_2 yield in this period can be associated with the selective catalyst deactivation for the reforming reactions involving oxygenates over their combustion, which seem to be affected by deactivation later.

Nevertheless, the evolution of CO yield with time on stream has a different trend, because it slightly increases between 0-200 min time on stream and subsequently it is almost constant. The initial increase can be linked to the fast deactivation of WGS reaction, which is coherent with the slight decrease in CO_2 yield in this period. The fact that CO yield remains almost constant after 200 min evidences that it is an intermediate product in the reaction kinetic scheme, and that deactivation attenuates both the individual reactions for its formation (reforming reactions) and its conversion (WGS and oxidation to CO_2).

It should be pointed out that, for 600 min, the bio-oil conversion is 0.83 and the yields of H_2, CO_2 and CO are 0.3, 0.63 and 0.05, respectively. These results are different to those corresponding to the thermal routes (Figure 2a), and prove that although the catalyst is almost totally deactivated for reforming reactions (especially of CH_4 and hydrocarbons), it keeps a remaining activity for WGS reaction, which should be attributed to the activity of CeO_2 in the support for WGS reaction [58].

3.4. Reaction scheme

The afore mentioned results give evidence of the difficulty for understanding the effect of reaction conditions on products yield in the OSR of raw bio-oil, due to the co-existence of thermal reactions with catalytic reactions, and to the role of the O_2 in the feed as a reactant. This difficulty is increased by the effect of catalyst deactivation on products yield.

The results of the runs without catalyst have proven that the extent of reforming reactions is insignificant in the 600-750 ºC range, and bio-oil conversion takes place mainly by decomposition and combustion of the oxygenates in bio-oil. Temperature has a significant effect on the extent of these reactions, so that the combustion reactions (mainly incomplete and with formation of CO, for low O/C ratio in the feed) have a higher relative significance when temperature is increased. Under conditions with high O_2 concentration (Figure 2b, at O/C = 0.67), the main route is the complete combustion of bio-oil oxygenates, as well as of the products of their decomposition (CH_4, hydrocarbons and CO), with CO_2 as major product.

The presence of catalyst attenuates the extent of the thermal routes of decomposition/cracking, by activating the catalyzed reactions of reforming, combustion and WGS.

The reaction conditions, and specially the space time (Figure 3), have a great effect on the relative importance of both groups of reactions. It is remarkable that Rh/ZDC catalyst used is very active and, consequently, at a moderate temperature (600 ºC) and with low space time value (0.15 $g_{catalyst}h/g_{bio\text{-}oil}$) high H_2 yield is achieved (up to 0.92) with low CO yield (0.035). These results are noticeably better than those obtained in the OSR of bio-oil with a Ni catalyst under reaction conditions similar to those used in this work [49].

Moreover, the O/C ratio (Figure 5) and, to a lower extent, the S/C ratio (Figure 6) affect noticeably the products yield, especially that of H_2. Thus, H_2 yield decreases almost linearly with O/C ratio (down to 0.6 for autothermal conditions) due to the promotion of combustion reactions. On the contrary, the increase in S/C ratio in the 3-9 range is efficient for increasing H_2 yield (and decreasing those of CO and CH_4), although this effect is attenuated above S/C = 6.

In order to have an overall view, the effect each reaction condition has on the yields of products in the OSR of bio-oil has been expressed with positive and negative signs in Table 1. Concerning H_2 yield, it can be stated that (from lower to higher effect) the increase in this yield is favored by increasing space time and S/C ratio, and it is disfavored by increasing temperature and more noticeably by increasing O/C ratio. However, other important factors to take into account for delimiting the suitable reaction conditions are the concentration of CO (which should be minimized for using the H_2 stream in fuel cells), the energy requirement and the catalyst cost (both being key factors for determining the cost of the process). The effect of reaction conditions on these factors is different to their effect on H_2 yield, so that the energy requirement increases with temperature and S/C ratio, and decreases when increasing O/C ratio. Moreover, the catalyst cost increases with space time, although this cost will also depend on catalyst deactivation (whose detailed study is out of the scope of this work). Consequently, these opposed effects should be taken into account in order to achieve a compromise between the criteria of H_2 production, CO concentration and costs. The results in this work are useful for approaching this objective, but a kinetic model is required for reactor simulation and optimization of reaction conditions.

Table 1

The mechanism and conversion pathway of bio-oil to CO_x and H_2 by reforming processes is complex due to the variety of the chemical compounds present in the bio-oil. Previous knowledge on this mechanism has been approached from studies with pure oxygenates such as ethanol [59-61] or with model compounds of oxygenate families in bio-oil, such as acetic acid or phenol [9,13,62-64]. According to Hung et al [60], there are three reaction pathways for OSR of ethanol, depending on the metal in the catalyst: ethanol can be oxidized to acetaldehyde (on Cu, Ag and Au), it can be dehydrated to ethylene (on Co, Ni, Pd and Pt), or it preferentially breaks its C-C bond and is further oxidized to CO or CO_2 on Ru, Rh and Ir, thus providing optimal H_2 production. Chen et al. [13] have proposed a reaction system for SR of acetic acid with primary reactions (catalyzed and thermal) and secondary reactions (catalyzed). In primary reactions, under catalytic effect of active metals acetic acid reacts with steam to form hydrogen, whereas thermal decomposition (which could happen with or without catalyst) mainly exists in three ways (to produce (CH_2CO+H_2O), ($CO+H_2$) or (CH_4+CO_2). Moreover, ketonization reaction forming acetone might exist with an enough acidic support. The secondary reactions mainly involve WGS reaction and further steam reforming of intermediate products (CH_4 and acetone). The proposed reaction mechanism for the steam reforming of phenol over Rh catalysts describes the dissociation of phenol on the metal particle leading to adsorbed hydrocarbon fragments, whereas the water molecule is activated on the support [62-64]. The resulting hydroxyl groups migrate to the metal particles through the metal/support interface which react with hydrocarbon fragments towards CO, CO_2 and H_2 formation. These contributions are of high interest in order to understand the mechanism of the steam reforming of pure compounds. However, due to the complex nature of bio-oil (consisting of oxygenate families with different

reactivity), the reaction mechanisms of pure oxygenates do not to apply in the case of bio-oil. Besides the complexity of the bio-oil itself, combustion reactions taking place in the oxidative steam reforming due to the presence of O_2 also hinder the formulation of a detailed reaction mechanism.

Consequently, in order to progress towards the proposal of a kinetic model, a reaction scheme is proposed for the OSR of bio-oil with Rh/ZDC catalyst, which is based on the afore-mentioned results involving the effect reaction conditions have on products yields (Figure 8). In this scheme, the thermal reactions (decomposition and combustion) and catalytic reactions (reforming, combustion and WGS) are considered, and also the relationship between the compounds in the reaction medium (except water). The scheme considers bio-oil conversion by means of: i) reforming (to form $CO+H_2$); ii) descomposition (to form CO, CO_2, CH_4, HCs and H_2), and; iii) combustion (to form CO, CO_2 and H_2O). CH_4 and light hydrocarbons are reformed with excess water to form CO and H_2. CO is converted by combustion to CO_2 and also by WGS reaction to form $CO_2 + H_2$. As this is an exothermic reversible reaction, the r-WGS reaction is promoted by the increase in temperature, thus producing CO and water from CO_2 and H_2. Although CH_4 reforming is also a reversible reaction, its reverse reaction (methanation) is not promoted at the high temperatures studied [32].

Figure 8

4. Conclusions

Rh/CeO_2-ZrO_2 catalyst shows a good performance in bio-oil OSR in a fluidized bed reactor. The pyrolytic lignin has been removed previously by polymerization of phenolic compounds at 500 ºC. This catalyst attains total conversion in OSR of bio-oil in the whole range of reaction conditions studied (600-750 ºC; space time, 0.15-0.6

$g_{catalyst}h/g_{bio-oil}$; S/C ratio, 3-9; O/C ratio, 0-0.67), with maximum H_2 yield of 0.92 and with low CO yield and insignificant CH_4 and hydrocarbons yields. O/C ratio is the variable with the highest effect on H_2 yield (which varies between 0.92-0.60 for O/C ratios between 0-0.67).

A kinetic scheme has been established based on the effect reaction conditions (with and without catalyst) have on products distribution. This kinetic scheme considers the thermal and the catalytic reactions in the OSR of bio-oil and the relationship between the compounds in the reaction medium, and explains the significance of reaction conditions on products yields.

The deactivation of the catalyst selectively affects the catalytic reactions according to this order: CH_4 reforming, hydrocarbons reforming, oxygenates reforming, combustion and WGS reaction. This information and the reaction scheme are useful for a future proposal of a kinetic model for the optimization of bio-oil OSR.

Acknowledgements

This work was carried out with the financial support of the Department of Education Universities and Investigation of the Basque Government (IT748-13), the University of the Basque Country (UFI 11/39 and Remiro's Postdoctoral grant) and the Ministry of Economy and Competitiveness of the Spanish Government jointly with the European Regional Development Funds (EDRF) (Proyects CTQ2012-35263 and CTQ2015-68883-R and Ph.D. grant BES-2013-063639 for A. Arandia).

References

[1] Ellabban O, Abu-Rub H, Blaabjerg F. Renewable energy resources: Current status, future prospects and their enabling technology, Renew Sust Energy Rev 2014;39:748-764.

[2] Moliner R, Lazaro, MJ, Suelves I. Analysis of the strategies for bridging the gap towards the Hydrogen Economy, Int J Hydrogen Energy 2016;41:19500-19508.

[3] Sgobbi A, Nijs W, De Miglio R, Chiodi A, Gargiulo M, Thiel C, How far away is hydrogen? Its role in the medium and long-term decarbonisation of the European energy system. Int J Hydrogen Energy 2016;41:19–35.

[4] Levalley TL, Richard AR, Fan M. The progress in water gas shift and steam reforming hydrogen production technologies - A review. Int J Hydrogen Energy 2014;39:16983-17000.

[5] Dincer I, Acar C. Review and evaluation of hydrogen production methods for better sustainability. Int J Hydrogen Energy 2015;40:11094-11111.

[6] Parthasarathy P, Narayanan KS. Hydrogen production from steam gasification of biomass: Influence of process parameters on hydrogen yield – A review. Renew Energy 2014;66:570-579.

[7] Eroglu E, Melis A. Microalgal hydrogen production research. Int J Hydrogen Energy 2016;41:12772-12798.

[8] Sarkar S, Kumar A, Large scale biohydrogen production from bio-oil. Bioresour Technol. 2010;101:7350–7361.

[9] Nabgan W, Tuan Abdullah TA, Mat R, Nabgan B, Gambo Y, Ibrahim M, Ahmad A, Jalil AA., Triwahyono S, Saeh I. Renewable hydrogen production from bio-oil

derivative via catalytic steam reforming: An overview, Renew Sust Energy Rev 2017;79:347-357.

[10] Bridgwater AV. Review of fast pyrolysis of biomass and product upgrading, Biomass Bioenerg 2012;38:68-94.

[11] Meier D, van de Beld B, Bridgwater AV, Elliott DC, Oasmaa A, Preto F. State-of-the-art of fast pyrolysis in IEA bioenergy member countries. Renew Sust Energ Rev 2013;20:619–641.

[12] Carpenter D, Westover TL, Czernik S, Jablonski W.. Biomass feedstocks for renewable fuel production: A review of the impacts of feedstock and pretreatment on the yield and product distribution of fast pyrolysis bio-oils and vapors. Green Chem 2014;16:384−406.

[13] Chen G, Tao J, Liu C, Yan B, Li W, Li X. Hydrogen production via acetic acid steam reforming: A critical review on catalysts. Renew Sust Energ Rev 2017;79:1091–1098.

[14] Zhang Y, Brown TR, Hu G, Brown RC.. Comparative techno-economic analysis of biohydrogen production via bio-oil gasification and bio-oil reforming. Biomass Bioenerg 2013;51:99–108.

[15] Xie H, Yu Q, Zuo Z, Han Z, Yao X, Qin Q. Hydrogen production via sorption-enhanced catalytic steam reforming of bio-oil. Int J Hydrogen Energy 2016;41:2345–235.

[16] Li D, Li X, Gong J. Catalytic reforming of oxygenates: state of the art and future prospects. Chem Rev 2016;116:11529–11653.

[17] Remiro A, Valle B, Aguayo AT, Bilbao J. Gayubo AG. Steam reforming of raw bio-oil in a fluidized bed reactor with prior separation of pyrolytic lignin. Energy Fuels 2013;27:7549–7559

[18] Remiro A, Valle B, Aramburu B, Aguayo AT, Bilbao J, Gayubo AG. Steam reforming of the bio-oil aqueous fraction in a fluidized bed reactor with in situ CO_2 capture. Ind Eng Chem Res 2013;52:17087–17098.

[19] Hajjaji N, Pons MN, Hydrogen production via steam and autothermal reforming of beef tallow: A thermodynamic investigation. Int J Hydrogen Energy 2013;38:2199–2211.

[20] Remiro A, Valle B, Aguayo AT, Bilbao J, Gayubo AG. Operating conditions for attenuating $Ni/La_2O_3–\alpha Al_2O_3$ catalyst deactivation in the steam reforming of bio-oil aqueous fraction. Fuel Process Technol 2013;115:222–232.

[21] Chattahathan SA, Adhikari A, Abdoulmoumine N. A review on current status of hydrogen production from bio-oil. Renew Sust Energ Rev 2012;16:2366–2372.

[22] Czernik S, French R, Distributed production of hydrogen by auto-thermal reforming of fast pyrolysis bio-oil. Int J Hydrogen Energy 2014;39:744–750.

[23] Paasikallio V, Azhari A, Kihlman J, Simell P, Lehtonen J. Oxidative steam reforming of pyrolysis oil aqueous fraction with zirconia pre-conversion catalyst. Int J Hydrogen Energy 2015;40:12088–12096.

[24] Medrano JA, Oliva M, Ruiz J, García L, Arauzo J. Catalytic steam reforming of acetic acid in a fluidized bed reactor with oxygen addition. Int J Hydrogen Energy 2008;33: 4387–4396.

[25] Trane R, Dahl S, Skjoth-Rasmussen MS, Jensen AD, Catalytic steam reforming of bio-oil. Int J Hydrogen Energy 2012;37:6447–6472.

[26] Vagia EC, Lemonidou AA, Thermodynamic analysis of hydrogen production via autothermal steam reforming of selected components of aqueous bio-oil fraction. Int J Hydrogen Energy 2008;33:2489–2500.

[27] Malaibari O, Amin A, Croiset E, Epling W. Performance characteristics of Mo-Ni/Al_2O_3 catalysts in LPG oxidative steam reforming for hydrogen production. Int J Hydrogen Energy 2014; 39:10061–10073.

[28] Silva PP, Ferreira RAR, Noronha FB, Hori CE. Hydrogen production from steam and oxidative steam reforming of liquefied petroleum gas over cerium and strontium doped $LaNiO_3$ catalysts. Catal Today 2016;289:211–221.

[29] Youn MH, Seo JG, Cho KM, Park S, Park DR, Jung JC, Song IK, Hydrogen production by auto-thermal reforming of ethanol over nickel catalysts supported on Ce-modified mesoporous zirconia: Effect of Ce/Zr molar ratio. Int J Hydrogen Energy 2008;33:5052–5059.

[30] Hu X, Lu G. Comparative study of alumina-supported transition metal catalysts for hydrogen generation by steam reforming of acetic acid. Appl Catal B-Environ 2010;99:289–297.

[31] Kamonsuangkasem K, Therdthianwong S, Therdthianwong A. Hydrogen production from yellow glycerol via catalytic oxidative steam reforming. Fuel Process Technol 2013;106:695–703.

[32] Vicente J, Ereña J, Montero C, Azkoiti MJ, Bilbao J, Gayubo AG. Reaction pathway for ethanol steam reforming on a Ni/SiO_2 catalyst including coke formation. Int J Hydrogen Energy 2014;39:18820–18834.

[33] Vicente J, Montero C, Ereña J, Azkoiti MJ, Bilbao J, Gayubo AG. Coke deactivation of Ni and Co catalysts in ethanol steam reforming at mild

temperatures in a fluidized bed reactor. Int J Hydrogen Energy 2014;39:12586–12596.

[34] Kechagiopoulos PN, Voutetakis SS, Lemonidou AA, Vasalos IA. Hydrogen Production via Reforming of the Aqueous Phase of Bio-Oil over Ni/Olivine Catalysts in a Spouted Bed Reactor. Ind Eng Chem Res 2009;48:1400–1408.

[35] Bimbela F, Oliva M, Ruiz J, García L, Arauzo J. Hydrogen production via catalytic steam reforming of the aqueous fraction of bio-oil using nickel-based coprecipitated catalysts. Int J Hydrogen Energy 2013;38:14476–14487.

[36] Salehi E, Seyedeyn-Azad F, Harding T, Abedi J. Production of hydrogen by steam reforming of bio-oil over Ni/Al_2O_3 catalysts: Effect of addition of promoter and preparation procedure. Fuel Process Technol 2011;92:2203–2210.

[37] Seyedeyn-Azad F, Abedi J, Harding T. Production of hydrogen via steam reforming of bio-oil over Ni-based catalysts: Effect of support. Chem Eng J 2012;180:145–150.

[38] Liguras DK, Kondarides DI, Verykios XE. Production of hydrogen for fuel cells by steam reforming of ethanol over supported noble metal catalysts. Appl Catal B-Environ 2003;43:345−54.

[39] Fierro V, Akdim O, Provendier H, Mirodatos C, Ethanol oxidative steam reforming over Ni-based catalysts. J Power Sources 2005;145:659–666.

[40] Chen H, Yu H, Tang Y, Pan M, Yang G, Peng F, et al. Hydrogen production via autothermal reforming of ethanol over noble metal catalysts supported on oxides. J Nat Gas Chem 2009;18:191–198.

[41] Chiodo V, Fredi S, Galvagno A, Mondello N, Frusteri, F. Catalytic features of Rh and Ni supported catalysts in the steam reforming of glycerol to produce hydrogen. Appl Catal A-Gen 2010;381:1–7.

[42] Gutierrez A, Karinen R, Airaksinen S, Kaila R, Krause A.O.I. Autothermal reforming of ethanol on noble metal catalysts. Int J Hydrogen Energy 2011;36: 8967–8977.

[43] Graschinsky C, Lupiano-Contreras J, Amadeo N, Laborde M. Ethanol oxidative steam reforming over Rh(1%)$MgAl_2O_4Al_2O_3$ catalyst. Ind Eng Chem Res 2014;53:15348-15356.

[44] Osorio-Vargas P, Campos CH, Navarro RM, Fierro JLG, Reyes P. Improved ethanol steam reforming on Rh/Al_2O_3 catalysts doped with CeO_2 or/and La_2O_3: Influence in reaction pathways including coke formation. Appl Catal A-Gen 2015;505:159–172.

[45] Sharma PK, Saxena N, Roy PK, Bhatt A. Hydrogen generation by ethanol steam reforming over Rh/Al_2O_3 and $Rh/CeZrO_2$ catalysts: A comparative study. Int J Hydrogen Energy 2016;41:6123–6133.

[46] Mondal T, Pant KK, Dalai AK. Catalytic oxidative steam reforming of bio-ethanol for hydrogen production over Rh promoted Ni/CeO_2-ZrO_2 catalyst. Int J Hydrogen Energy 2015;40:2529–2544.

[47] Rioche C, Kulkarni S, Meunier FC, Breen JP, Burch R. Steam reforming of model compounds and fast pyrolysis bio-oil on supported noble metal catalysts. Appl Catal B-Environ 2005;61:130–139.

[48] Rennard D, French R, Czernik S, Josephson T, Schmidt L. Production of synthesis gas by partial oxidation and steam reforming of biomass pyrolysis oils. Int J Hydrogen Energy 2010;35:4048–4059.

[49] Remiro A, Arandia A, Bilbao J, Gayubo AG. Comparison of Ni Based and Rh Based Catalyst Performance in the Oxidative Steam Reforming of Raw Bio-Oil. Energy Fuels 2017;31:7147–7156.

[50] Gayubo AG, Valle B, Aguayo AT, Olazar M, Bilbao J. Pyrolytic lignin removal to valorise biomass pyrolysis crude bio-oil by catalytic transformation. J Chem Technol Biotechnol 2010;85:132–144.

[51] Valle B, Remiro A, Aramburu B, Bilbao J, Gayubo AG. Strategies for maximizing the bio-oil valorization by catalytic transformation. J Clean Prod 2015;88:345–348.

[52] Fernandez-Akarregi AR, Makibar J, Lopez G, Amutio M, Olazar M. Design and operation of a conical spouted bed reactor pilot plant (25 kg/h) for biomass fast pyrolysis. Fuel Process Technol 2013;112:48–56.

[53] Amutio M, Lopez G, Artetxe M, Elordi G, Olazar M. Influence of temperature on biomass pyrolysis in a conical spouted bed reactor. Resour Conserv Recy 2012;59:23–31.

[54] Amutio M, Lopez G, Aguado R, Artetxe M, Bilbao J, Olazar M. Kinetic study of lignocellulosic biomass oxidative pyrolysis. Fuel 2012;95:305–311.

[55] Arandia A, Remiro A, Valle B, Bilbao J, Gayubo A.G. Operating strategies for the oxidative steam reforming (OSR) of raw bio-oil in a continuous two-step system. Chem Eng Trans 2017;57:217–222.

[56] Vicente J, Ereña J, Oar-Arteta L, Olazar M, Bilbao J, Gayubo AG. Effect of operating conditions on DME steam reforming in a fluidized bed reactor with a CuO-ZnO-Al_2O_3 and desilicated ZSM-5 zeolite bifunctional catalyst. Ind Eng Chem Res 2014;53:3462–3471.

[57] Valle B, Aramburu B, Benito PL, Bilbao J, Gayubo AG. 2017. Biomass to hydrogen-rich gas via steam reforming of raw bio-oil over Ni/La_2O_3-Al_2O_3 catalyst: Effect of space-time and steam-to-carbon ratio, Fuel 2017 submitted.

[58] Roh H-S, Potdar HS, Jeong D-W, Kim K-S, Shim J-O, Jang W-J, Koo KY, Yoon, WL. Synthesis of highly active nano-sized (1 wt.% Pt/CeO_2) catalyst for Water Gas Shift reaction in medium temperature application. Catal Today 2012;185:113–118.

[59] de Lima SM, da Silva AM, da Costa LOO, Graham UM, Jacobs G, Davis BH, Mattos LV, Noronha FB. Study of catalyst deactivation and reaction mechanism of steam reforming, partial oxidation and oxidative steam reforming of ethanol over Co/CeO_2 catalyst. J Catal. 2009;268:268-281.

[60] Hung C-C, Chen S-L, Liao Y-K, Chen C-H, Wang J-H. Oxidative steam reforming of ethanol for hydrogen production on M/Al_2O_3. Int J Hydrogen Energy 2012;27:4955-4966.

[61] Xu W, Liu Z, Johnson-Peck AC, Senanayake SD, Zhou G, Stacchiola D, Stach EA, Rodriguez JA. Steam reforming of ethanol on Ni/CeO_2: Reaction pathway and interaction between Ni and CeO_2 support. ACS Catal 2013;3:975-984.

[62] Polychronopoulou K, Efstathiou AM, Spillover of labile OH, H, and O species in the H production by steam reforming of phenol over supported-Rh catalysts. Catal Today 2006;116:341-347.

[63] Polychronopoulou K, Costa CN, Efstathiou AM. The role of oxygen and hydroxyl support species on the mechanism of H production in the steam reforming of phenol over metal oxide-supported-Rh and -Fe catalysts. Catal Today 2006;112:89-93.

[64] Constantinou DA, Álvarez-Galván MC, Fierro JLG, Efstathiou AM. Low-temperature conversion of phenol into CO, CO_2 and H_2 by steam reforming over La containing supported Rh catalysts. Appl Catal B-Environ 2012;117–118:81–95.

Figure Captions

Figure 1. TEM image of Rh/ZDC catalyst after reduction and particle size distribution (inserted window).

Figure 2. Effect of temperature (a) and O/C ratio (b) on bio-oil conversion and products yields by thermal routes (without catalyst). Reaction conditions: S/C ratio, 6. Graph a: O/C ratio, 0.34 and 0. Graph b: 700 ºC.

Figure 3. Effect of space time on bio-oil conversion and products yields at 600 ºC (a) and 700 ºC (b). Reaction conditions: O/C ratio, 0.34; S/C ratio, 6.

Figure 4. Effect of temperature on bio-oil conversion and products yields, for space time of 0.6 $g_{catalyst}h/g_{bio\text{-}oil}$ (a) and 0.15 $g_{catalyst}h/g_{bio\text{-}oil}$ (b). Reaction conditions: O/C ratio, 0.34; S/C ratio, 6.

Figure 5. Effect of O/C molar ratio on bio-oil conversion and products yields at 600 ºC and 0.6 $g_{catalyst}h/g_{bio\text{-}oil}$ (a) and at 700 ºC and 0.15 $g_{catalyst}h/g_{bio\text{-}oil}$ (b). Reaction conditions: S/C ratio, 6.

Figure 6. Effect of S/C molar ratio on bio-oil conversion and products yields at 600 ºC and 0.6 $g_{catalyst}h/g_{bio\text{-}oil}$ (a) and at 700 ºC and 0.15 $g_{catalyst}h/g_{bio\text{-}oil}$ (b). Reaction conditions: S/C ratio, 6.

Figure 7. Evolution with time on stream of bio-oil conversion and yields of products. Reaction conditions: 600 ºC; space time, 0.6 $g_{catalyst}h/g_{bio\text{-}oil}$; O/C ratio, 0.34; S/C ratio, 6.

Figure 8. Reaction scheme for the OSR of bio-oil with Rh/ZDC catalyst.

Tables and Figures

Table 1. Qualitative effect of the increase in the different reaction conditions on the yields of products and costs (energy requirement and catalyst cost) in the OSR of bio-oil with Rh/ZDC catalyst.

		Temperature (600-750 ºC)	**Space time (0.15 – 0.60 $g_{catalyst}h/g_{bio\text{-}oil}$)**	**S/C ratio (3 – 9)**	**O/C ratio (0 – 0.67)**
Yield	H_2	–	+	++	– – –
	CO_2	–	+	+	++
	CO	+	–	–	–
	CH_4	–	–	–	–
	HCs	*	–	*	*
Costs		+	+	++	– – –

* Insignificant formation at zero time above 0.15 $g_{catalyst}h/g_{bio\text{-}oil}$

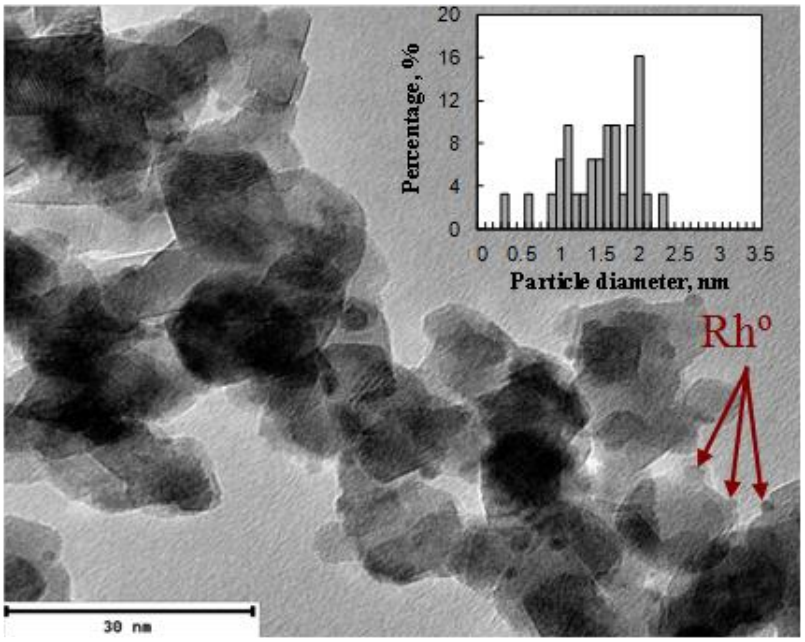
Percentage, %
20
16
12
8
4
0
0 0.5 1 1.5 2 2.5 3 3.5
Particle diameter, nm
Rh°
30 nm

Figure 1

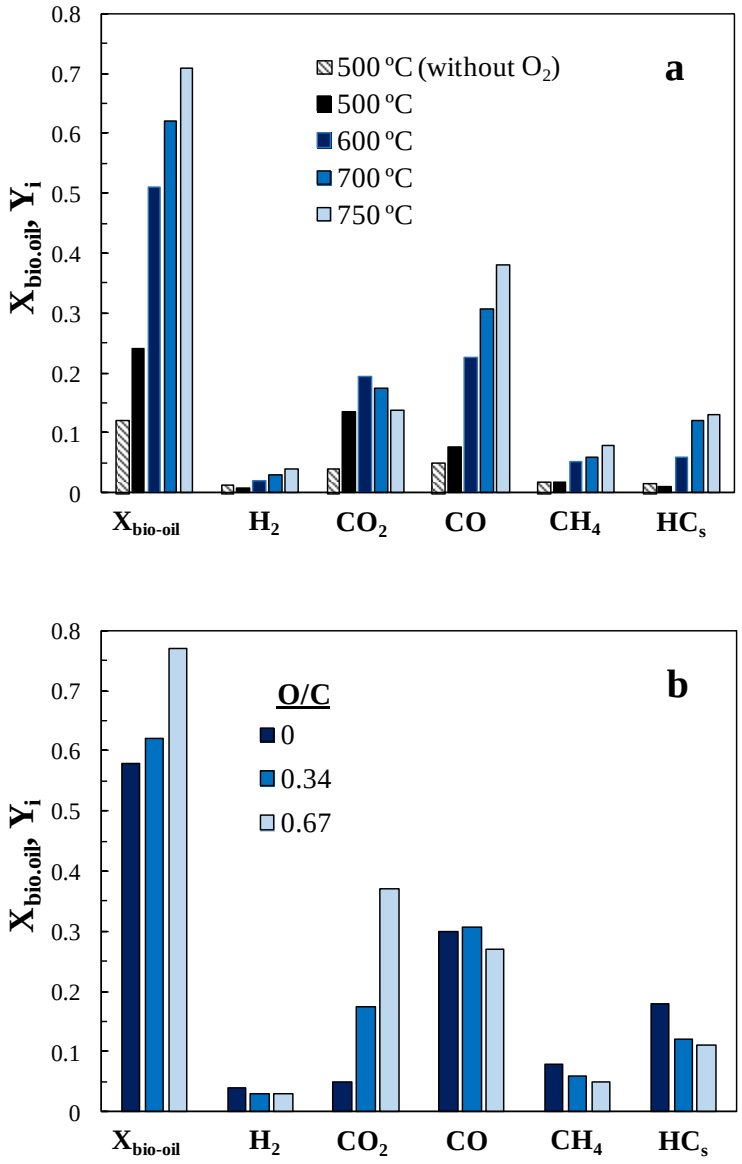
a
500 ºC (without O2)
500 ºC
600 ºC
700 ºC
750 ºC
Xbio-oil, Yi
0.8
0.7
0.6
0.5
0.4
0.3
0.2
0.1
0
Xbio-oil
H2
CO2
CO
CH4
HCs
b
O/C
0
0.34
0.67
Xbio-oil, Yi
0.8
0.7
0.6
0.5
0.4
0.3
0.2
0.1
0
Xbio-oil
H2
CO2
CO
CH4
HCs

Figure 2

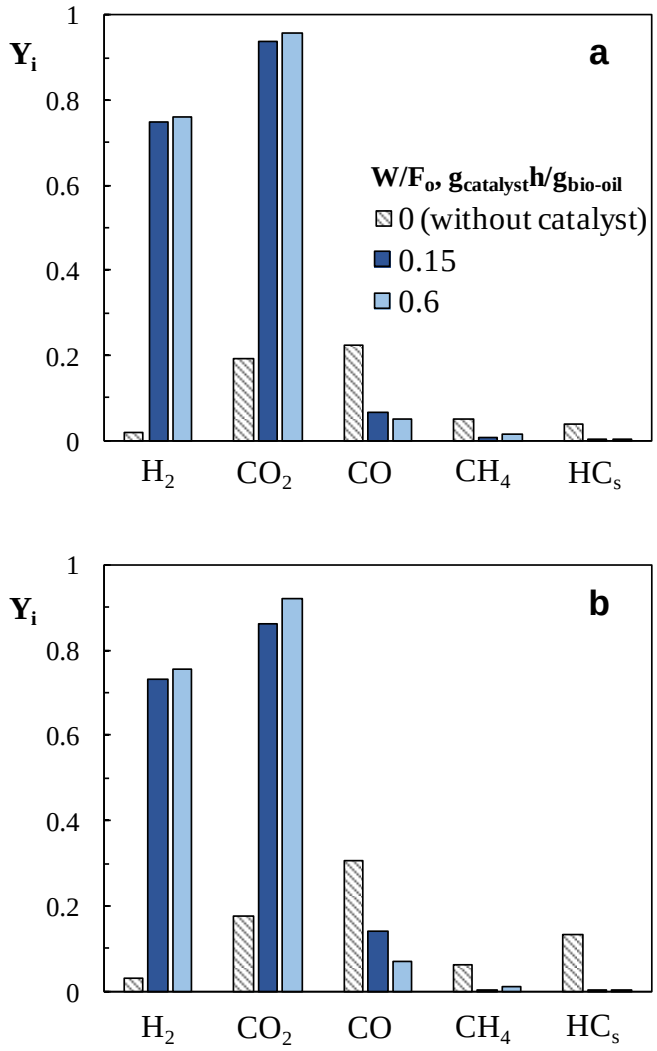
Y_i
a
W/F_o, g_catalyst h/g_bio-oil
0 (without catalyst)
0.15
0.6
1
0.8
0.6
0.4
0.2
0
H2
CO2
CO
CH4
HCs
b

Figure 3

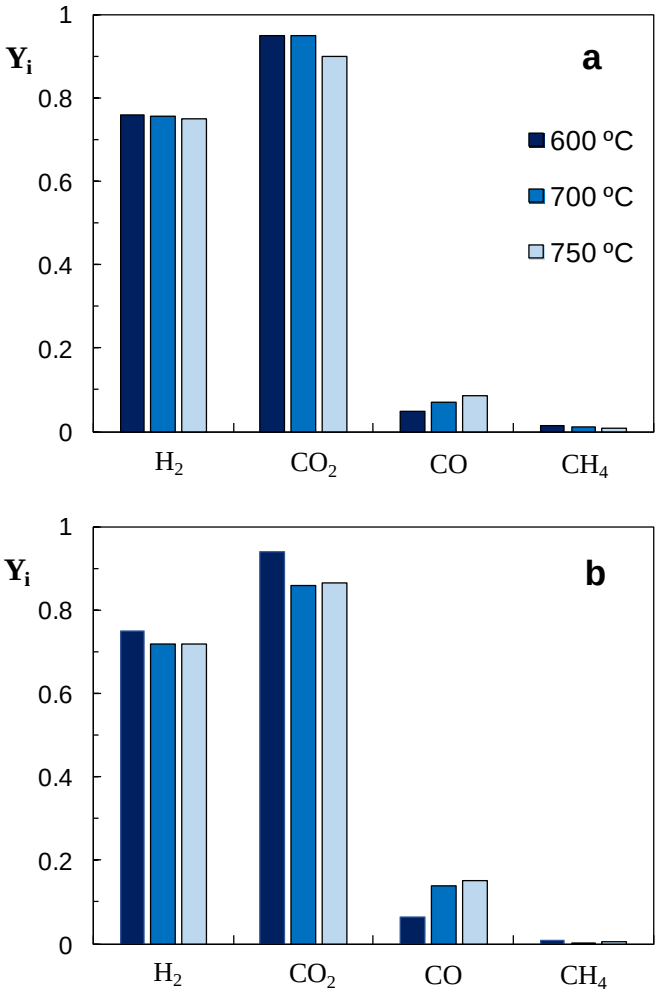
Yi
1
0.8
0.6
0.4
0.2
0
a
600 ºC
700 ºC
750 ºC
H2
CO2
CO
CH4
Yi
1
0.8
0.6
0.4
0.2
0
b
H2
CO2
CO
CH4

Figure 4

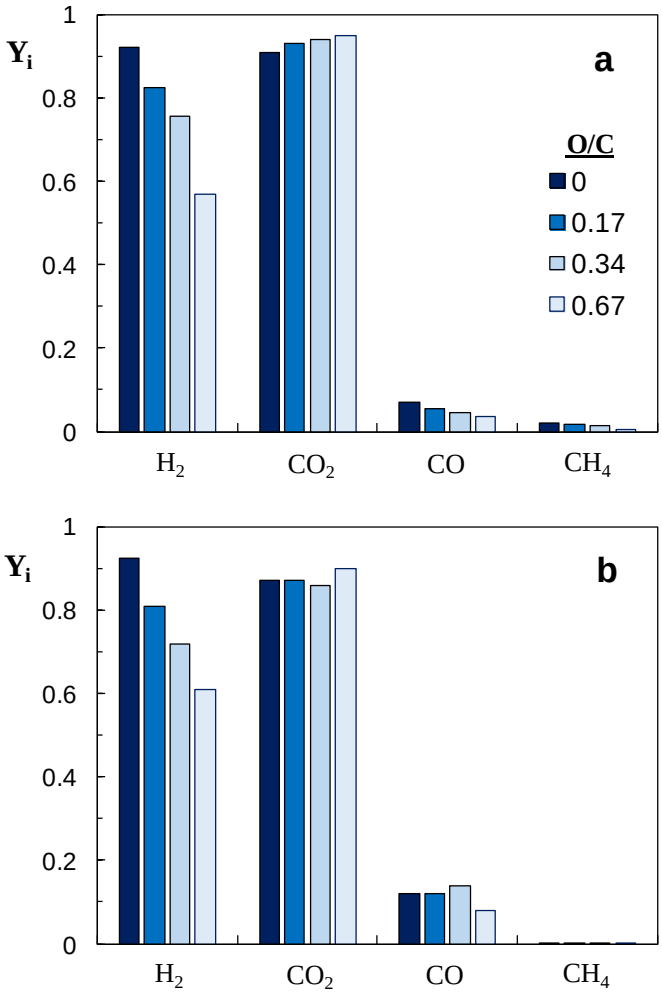
Yi
1
0.8
0.6
0.4
0.2
0
a
O/C
0
0.17
0.34
0.67
H2
CO2
CO
CH4
Yi
1
0.8
0.6
0.4
0.2
0
b
H2
CO2
CO
CH4

Figure 5

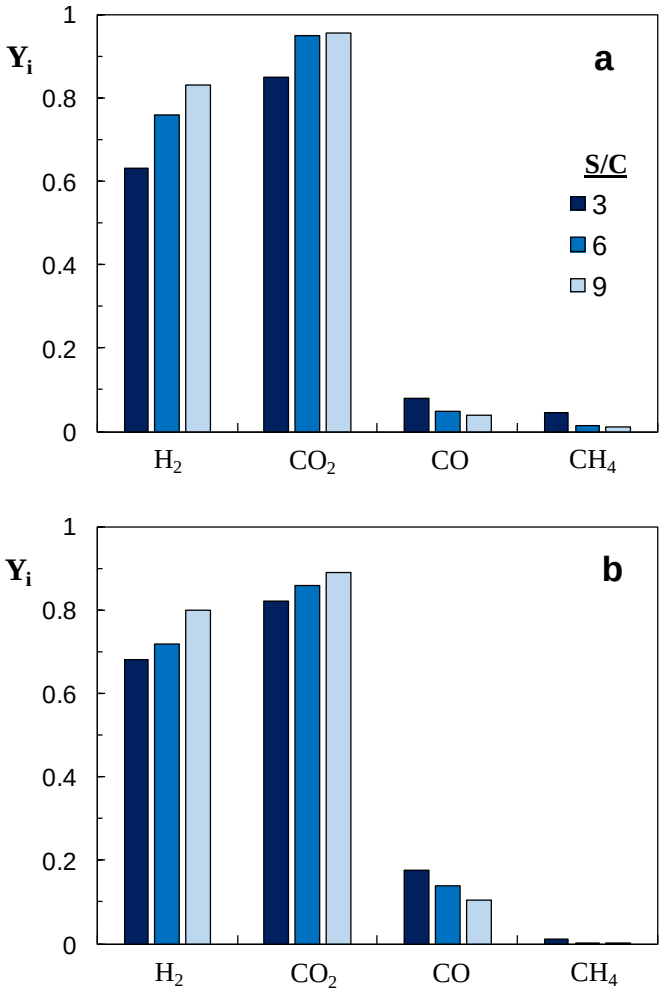
Y_i
1
0.8
0.6
0.4
0.2
0
a
S/C
3
6
9
H2
CO2
CO
CH4
Y_i
1
0.8
0.6
0.4
0.2
0
b
H2
CO2
CO
CH4

Figure 6

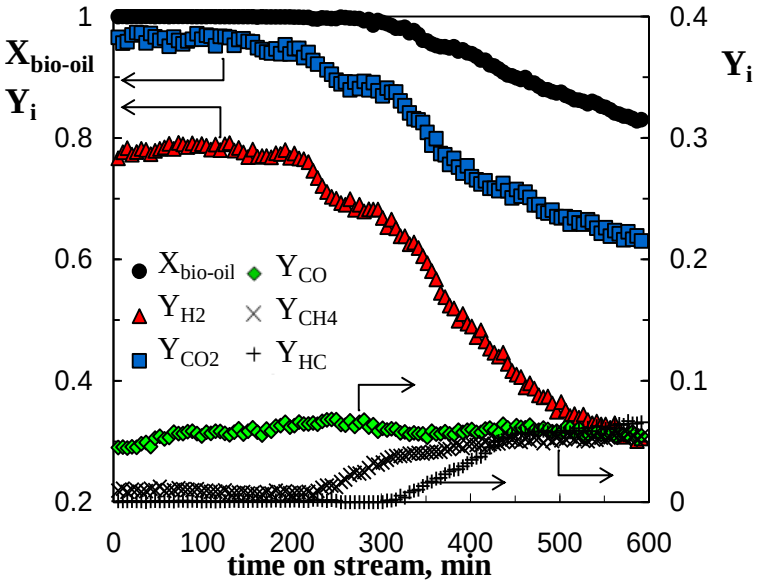
X bio-oil
Y i
Y i
1
0.8
0.6
0.4
0.2
0.4
0.3
0.2
0.1
0
X bio-oil
Y CO
Y H2
Y CH4
Y CO2
Y HC
0
100
200
300
400
500
600
time on stream, min

Figure 7

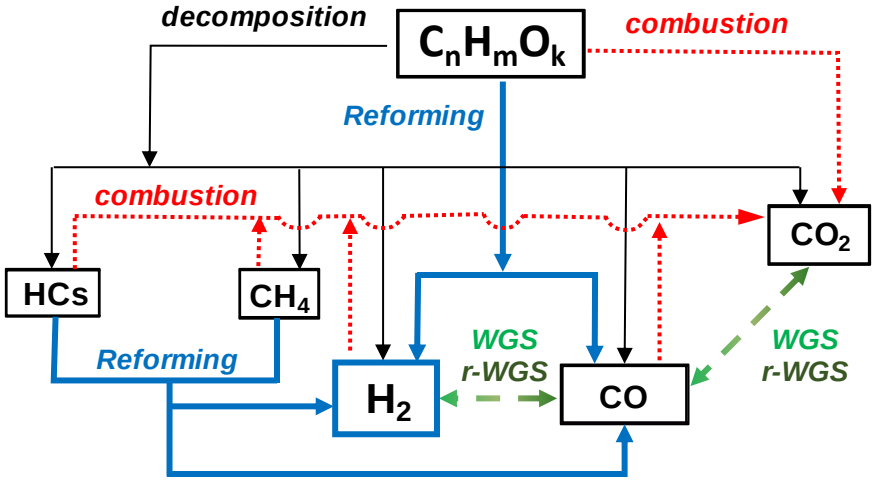
decomposition
$C_nH_mO_k$
combustion
Reforming
combustion
CO_2
HCs
CH_4
Reforming
WGS
r-WGS
WGS
r-WGS
H_2
CO

Figure 8